journal

J. Am. Ceram. Soc., 93 [3] 716–721 (2010)
DOI: 10.1111/j.1551-2916.2009.03478.x
© 2009 The American Ceramic Society

Sodium Fluoride Solubility and Crystallization in Photo-Thermo-Refractive Glass

Vladimir M. Fokin, Guilherme P. Souza,† and Edgar D. Zanotto

Vitreous Materials Laboratory (LaMaV), Department of Materials Engineering (DEMa), Federal University of Sao Carlos, 13565-905 Sao Carlos, SP, Brazil

Julien Lumeau, Larissa Glebova, and Leonid B. Glebov

CREOL, The College of Optics and Photonics, University of Central Florida, PO Box 162700, Orlando, Florida 32816-2700

Photo-thermo-refractive (PTR) glass undergoes a refractive index change after UV exposure followed by heat treatment for nanocrystallization of NaF, allowing phase holograms to be permanently recorded in the glass. PTR glass was invented 60 years ago, and optical elements based on PTR glass have been produced for the past decade, but its detailed crystallization mechanism is largely unknown. Since solubility and composition of the parent glass determine the supersaturation and hence the thermodynamic driving force for crystallization, the present paper was aimed at measuring the solubility of NaF in PTR glass via estimating the equilibrium volume fraction of crystallized NaF as a function of temperature. The temperature above which all NaF originally contained in the parent glass remains dissolved in the melt, and that below which all NaF could crystallize, were also estimated. Redesigning of thermal processing parameters and composition of PTR glass, aiming at the improvement of optical elements based on this glass, can be performed in light of the results achieved.

I. Introduction

PHOTO-THERMO-REFRACTIVE (PTR) glass undergoes a (local) refractive index change after UV exposure followed by proper heat treatment for nanocrystallization.[1] In this way, phase holograms can be permanently recorded in the bulk of the glass. Although coloration in glass resulting from photo-thermo-induced crystallization was first described by Stookey[2] about 60 years ago, it was only over the past 40 years that discovery of refractive index change after photo-thermal processing has led to a breakthrough in the photonics industry.[3] At present, high-efficiency volume diffractive optical elements (DOEs) made of PTR glass find a wide range of applications, which include, e.g. beam deflectors, splitters, and attenuators.[4]

From a chemical standpoint, PTR glass is a Na_2O–Al_2O_3–ZnO–K_2O–SiO_2 glass containing a few mol% Br and F, doped with Ce, Ag, Sb, and Sn. Refractive index change arises from volume crystallization of NaF nanocrystals, induced by exposure to a UV laser radiation followed by heat treatment. Despite the fact that optical elements based on PTR glass are currently produced, the crystallization mechanism and kinetics in this glass are largely unknown.

The following simplified scenario has been thought to take place during the photo-thermal processing of PTR glass: after absorbing a UV photon, Ce^{3+} is oxidized to Ce^{4+} releasing one electron that is trapped by a silver ion to form Ag^0. Then nano-sized clusters of metallic silver appear in the early stages of heat treatment and serve as nuclei for subsequent heterogeneous crystallization that finally leads to NaF formation. In DOEs, this is a simplified mechanism of crystallization for the UV-exposed regions. It should be noted that PTR glass without Ag and/or without UV exposure also undergoes (less intense) volume crystallization of NaF. Thus, the role of Ag and UV exposure is to boost NaF nucleation. Precipitation of NaF in fluorinated glasses, including PTR glass, has been known for a long time, e.g. Corning kitchenware. As mentioned above, the main role of UV exposure is to reinforce the NaF nucleation kinetics by generating of additional nucleation centers (after heat treatment), causing a decrease in the refractive index in the UV-exposed volume. Heat treatment is required to produce a large negative refractive index change (several hundreds of ppm) and the photo-thermo-refractivity of PTR glass requires the appearance of NaF crystals. A detailed study of the complex mechanisms involved can be found in Lumeau *et al.*[5] However, crystallization of NaF in the unexposed glass also causes decrease of refractive index, decreasing the relative refractive index change (defined as the difference of refractive index between UV-exposed and unexposed parts of the glass after heat treatment).

Moreover, liquid immiscibility should be considered when addressing phase transitions in PTR glass. In Souza *et al.*,[6] it was shown that a fine droplet-like structure resembling liquid-liquid phase separation, revealed after etching, appeared in heat-treated samples. Liquid immiscibility in sodium-silicate glasses is rather expected,[7] and is reinforced by the presence of fluorine in the glass,[8] which is the case of PTR glass.

A distinctive characteristic of crystallization in PTR glass is that the volume fraction of crystallized NaF is limited by two factors, which are the low ($\sim$5 mol%) sodium fluoride content in the original glass and the solubility of NaF. Crystallization of NaF in PTR glass is thus extremely nonstoichiometric, i.e. the composition of the crystals is completely different from that of the parent glass. This leads to depletion of the melt in Na and especially F upon crystallization of NaF, which is accompanied by an increase of the melt viscosity and glass transition temperature, T_g.[9,10] Diffusion of these two elements from the glass into the crystals results in marked diffusion zones around the NaF crystals, which were first reported in Souza *et al.*[6] Thus, the kinetics of NaF crystallization slows down as the composition of the glass matrix is progressively changed, as revealed by e.g. decrease of crystal growth until its complete halt. The problem of limited content of the crystallized component, such as NaF in PTR glass, is similar to the case of the crystallization of dopants

L. Pinckney—contributing editor

Manuscript No. 26568. Received July 28, 2009; approved October 2, 2009.
The work was supported by DARPA ADHELS program, contract HR-0011-06-1-0010, and by IMI/NFG, grant DMR-0409588.
†Author to whom correspondence should be addressed. e-mail: gparente003@hotmail.com

often used as catalysts for volume crystallization in glass–ceramics. Since the solubility of most solid phases in a melt increases with increasing temperature, dopants dissolved in a glass forming melt at high temperature will precipitate at a lower temperature if their concentration exceeds their solubility. Thus, the composition of the parent glass and the solubility of the crystalline phase are the critical issues governing the maximum crystallized fraction corresponding to the equilibrium between crystalline and liquid phases.

Several studies have been devoted to processes of dissolution and precipitation of crystals in glass forming melts of both natural and manufactured origins,[11–14] but none has been dedicated to PTR glass. The present paper aims at the study of NaF solubility in PTR glass. Solubility data are critical as they are needed for estimating the thermodynamic driving force for both crystal nucleation and growth, which in turn determine the number density and the size distribution of the precipitated crystalline phase.

II. Experimental Procedure

A PTR glass with composition $15Na_20$–$5ZnO$–$4Al_2O_3$–$70SiO_2$–$5NaF$–$1KBr$–$0.01Ag_2O$–$0.01CeO$–$0.01SnO_2$–$0.03Sb_2O_3$ (mol%) was prepared via melting at 1460°C, cooling to 460°C ($T_g \sim 473$°C) and annealing at this temperature for 1 h. The glass was not exposed to UV light. For isothermal treatments, glass samples not larger than 3 mm × 3 mm × 3 mm were dropped into a previously stabilized electric box furnace. Heat treatment temperatures ranged from 520° to 750°C. After a given period of time, samples were pulled out from the furnace and quenched in air to room temperature. The volume fraction of the crystallized phase (α) as a function of heat treatment temperature was measured by quantitative X-ray diffraction (XRD) analysis.[15] XRD measurements were carried out on powdered samples using a Siemens D5005 X-ray diffractometer (Siemens, Munich, Germany) operating at 40 mA and 40 kV. Cu$K\alpha$ (1.5406 Å) was used as incident radiation to scan samples from $36° \leq 2\theta \leq 41°$ at a scanning speed of 0.6°/min. A Leica DMRX optical microscope (Leica, Wetzlar, Germany) coupled with a Leica DFC490 CCD camera was used to investigate the morphology of crystals embedded in the glass. Both transmitted light and reflected light modes were applied. For transmitted light optical microscopy, thin (~150 μm) samples were prepared by cutting, grinding, and CeO_2 polishing. Sample preparation for both reflected light optical microscopy and scanning electron microscopy (SEM) involved etching with hydrofluoric acid (HF), which was applied to show key microstructural features. This procedure was detailed in Souza *et al.*[6] A Philips XL30 field emission gun SEM (Philips, Amsterdam, the Netherlands) was used for secondary electron (SE) imaging of phase assemblages and morphology on fractured surfaces of heat-treated samples. In this case a weak etching was applied (15 s instead of 2 min for the optical microscopy observations). A Netzsch 404 differential scanning calorimeter (Netzsch, Selb/Bavaria, Germany) was used to measure T_g of untreated as well as heat-treated glass samples, which were run in a platinum crucible at 10 K/min from room temperature until 650°C.

III. Results

Figure 1 shows optical micrographs of PTR glass after isothermal treatments at 650° and 700°C. The NaF crystals have a distinctive dendritic morphology. The crystal number density is higher for the sample with smaller crystals (heat treated at 650°C). Reflected light optical micrographs of etched samples reveal a very fine droplet structure in the glass matrix with size close to the resolution of our optical microscope (see inset in Fig. 1(a)). Such structure was only revealed after etching with HF, and could not be observed through the volume of the thin samples analyzed under transmitted light. In Souza *et al.*,[6] SEM

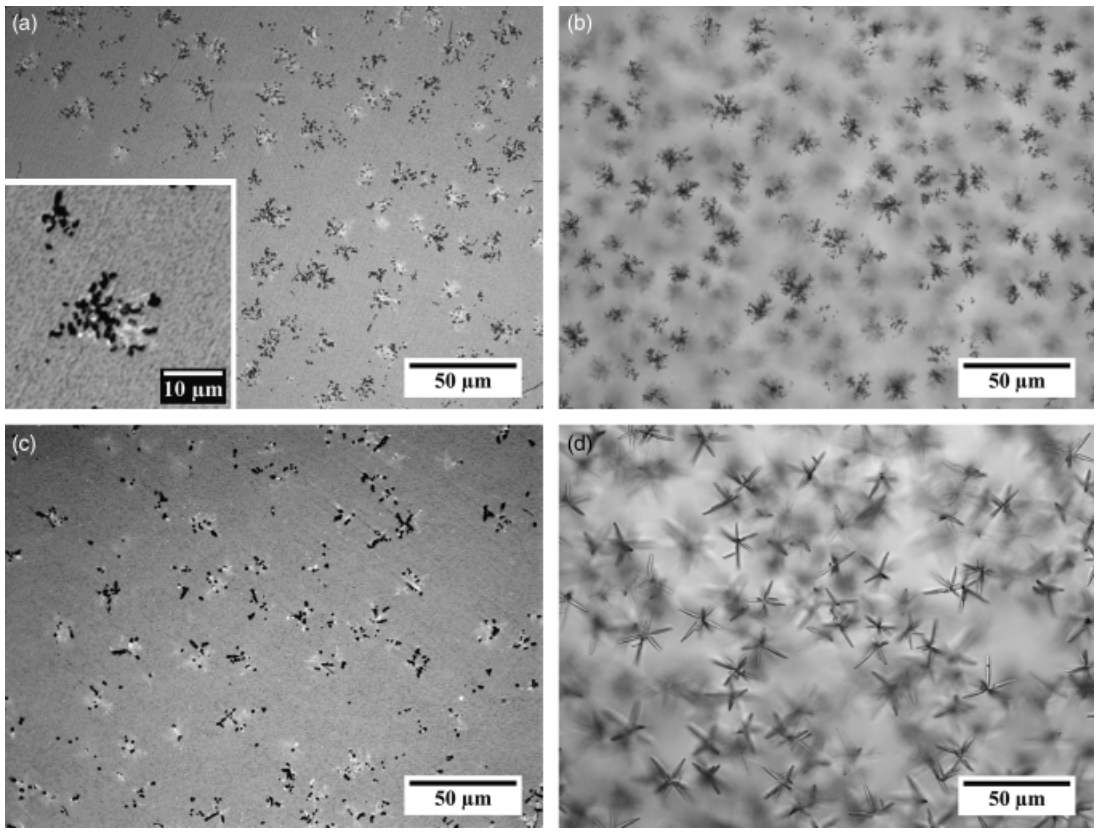

Fig. 1. Reflected light (a and c) and transmitted light (b and d) optical micrographs of PTR glass samples heat treated at 650°C for 2 h (a and b) and at 700°C for 30 min (c and d). The thickness of samples in (b) and (d) was ~150 μm. Fine structure is detailed in inset in (a).

was utilized to reveal the droplet-like morphology of this fine structure, which was related to liquid immiscibility. As the heat-treatment temperature is increased from 650° to 700°C, the shape of the dendrites turns to a more spiky morphology, with larger, elongated features. XRD analysis confirmed that crystals shown in Fig. 1 are NaF. XRD also detected NaBr crystals in small amounts compared with NaF, thus it is possible that a minor fraction of the crystallized microstructure comprises a mixture between NaF and NaBr, which does not interfere with the rationale of the present work. Heat-treatment times were chosen as those necessary to promote maximum volume fraction of NaF crystalline phase for each temperature, initially on the basis of microstructural observations. After some time at a given temperature, NaF crystallization halts due to the limited NaF content in the parent glass and its solubility.

Because the residual glassy matrix is depleted in fluorine and sodium due to formation of NaF crystals, an increase in the glass transition temperature T_g with increasing crystallized fraction α is expected.[9] Indeed, as shown in Fig. 2, T_g generally increases with increasing heat treatment time at 650°C, and hence increasing α, until reaching saturation, $T_{g/s}$ (T_g at saturation). Since the evolution of residual glass composition is determined by precipitation of NaF crystals it is reasonable to suppose that saturation of T_g is accompanied by saturation of crystallized fraction of NaF (α). It is important to note that, initially, T_g values pass through a minimum. As discussed in Souza *et al.*,[6] liquid–liquid phase separation occurs in PTR glass with a silica-rich, droplet-like phase. As the relative content of silica in the continuous glass matrix, surrounding the droplet phase, is lower than that in the parent (homogeneous) glass, one can expect a decrease of T_g of the glass matrix compared with the parent glass. On the other hand, depletion of fluorine and sodium in the glass matrix due to NaF crystallization results in an increase of glass transition temperature. Thus the minimum on the T_g–t plot (Fig. 2) should be caused by an interplay between crystallization and liquid–liquid phase separation. Enhancement of the overall crystallization kinetics via preliminary nucleation at 480°C accelerates the increase of T_g (stars in Fig. 2), eliminating or masking the minimum observed for the nonnucleated glass. As expected, the level of saturation of T_g, $T_{g/s}$, clearly does not depend on the nucleation step. It should also be noted that T_g of glass samples heat treated at 480°C for 35 min is slightly lower than that of the parent glass, annealed at 460°C upon glass melting. Such minor drop of T_g may have been caused by either structural relaxation (at 480° > 460°C) or liquid–liquid phase separation.

Other T_g–t plots, as the one shown in Fig. 2, were obtained for various heat treatment temperatures (520°–750°C). Those were used to estimate the heat treatment time needed for reaching a constant value of $T_{g/s}$, or the equilibrium between crystalline (NaF) and glassy phases. The equilibrium volume fraction of NaF crystals was then determined for each temperature. The heat treatment time necessary for reaching $T_{g/s}$ increases with decreasing the heat treatment temperature. $T_{g/s}$ as a function of temperature is shown in Fig. 3. Since, in the case of PTR glass, T_g is very sensitive to variations of melt composition due to NaF crystallization, we used this T_g variation to demonstrate that the displacement of equilibrium between crystalline (NaF) and glassy phases with temperature is a reversible process. Figure 4 shows a sequence of heat treatments and resulting values of T_g. Each isothermal treatment was carried out by inserting the glass sample into a previously stabilized furnace and quenching the sample in air to room temperature. The glass sample was first heat treated at $T = 680$°C for 1 h. T_g increased from 473°C (point 1 in Fig. 4 is T_g of the parent glass) to 482°C (point 2). This higher value of T_g corresponds to saturated (as regards to crystallized NaF) melt. The dashed line in Fig. 4 is a linear fit of experimental data $T_{g/s}$–T shown in Fig. 3. The same sample (partly crystallized PTR glass) was subsequently treated at a lower temperature $T = 570$°C for 12 h. This heat treatment

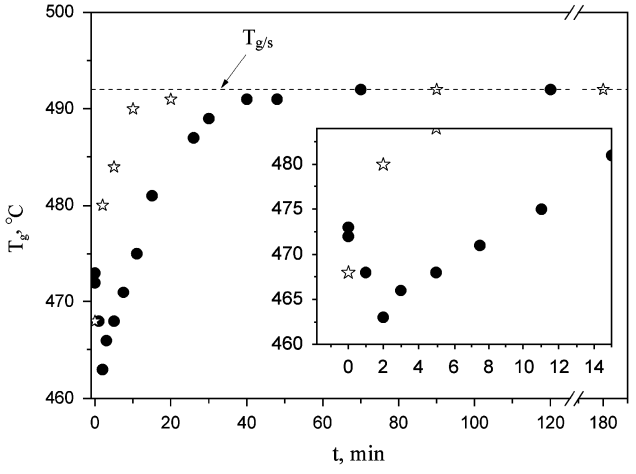

Fig. 2. T_g measured by differential scanning calorimeter as a function of heat treatment time at 650°C for the original samples (●) and for samples previously nucleated at 480°C for 35 min (★). The first 15 min of treatment are shown in detail (inset).

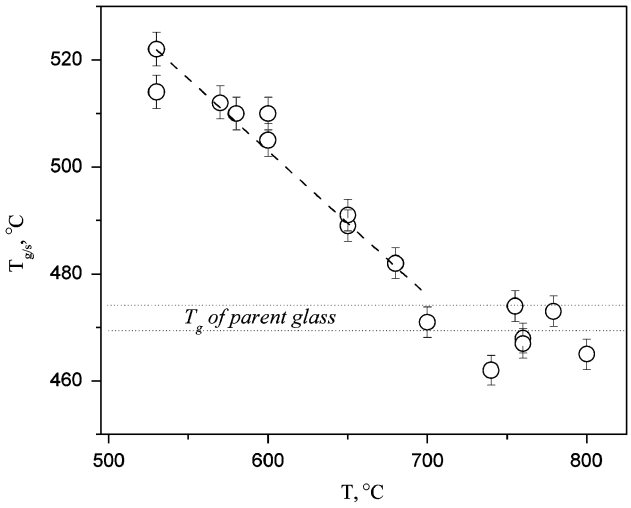

Fig. 3. Glass transition temperature at saturation ($T_{g/s}$) measured by differential scanning calorimeter as a function of heat treatment temperature. The heat treatment time for each isotherm corresponds to that of saturation of the T_g shift indicating maximum crystallized fraction of NaF for that temperature.

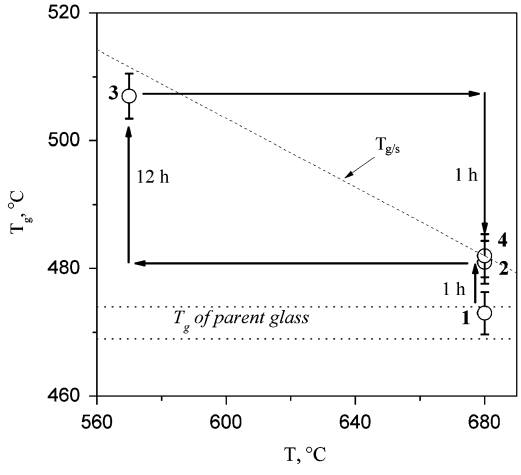

Fig. 4. Schematics of reversible change in glass transition temperature at saturation ($T_{g/s}$), measured by differential scanning calorimeter, as a function of heat treatment temperature. Points 1, 2, 3, and 4 correspond to: T_g of the untreated glass, $T_{g/s}$ of the same sample heat treated at 680°C for 1 h, $T_{g/s}$ after heat treatment at 570°C for 12 h, and $T_{g/s}$ of the same sample heat treated back at 680°C for 1 h, respectively.

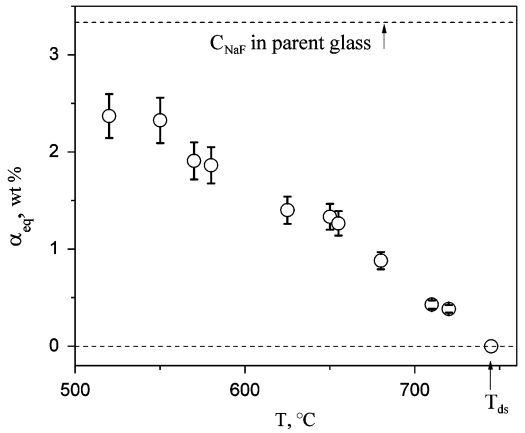

Fig. 5. Crystallized fraction (α) measured by quantitative X-ray diffraction as a function of heat treatment temperature. Heat treatment time for each isotherm corresponds to that of saturation of T_g shift, indicating maximum crystallized fraction of NaF for that temperature.

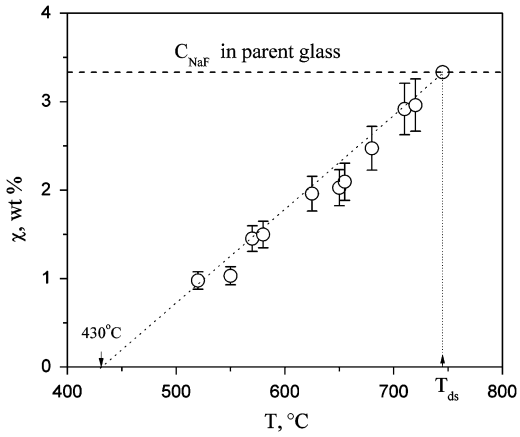

Fig. 6. Solubility in weight percent of NaF in the glass as a function of temperature.

resulted in relaxation of the system by the increase of crystallized volume and establishment of a new equilibrium state with the melt composition corresponding to $T_g = 510°C$ (point 3), which is reasonably close to the plotted $T_{g/s}$–T dashed line. A further heat treatment at $T = 680°C$ for 1 h shifts the system back to its initial equilibrium state at that temperature (point 4) through partial dissolution of (NaF) crystalline phase produced at a lower temperature. The results presented above give solid evidence for the reversibility of NaF crystal growth and dissolution processes in PTR glass.

To quantify the equilibrium volume fraction of crystallized NaF, α_{eq}, corresponding to each heat treatment temperature, the area S_{200} of the strongest diffraction peak (200) of NaF, obtained by XRD, was measured in each case. Areas were converted into α_{eq} via a calibration plot S_{200}–α obtained for (0, 5, 10, and 15 vol% NaF) powder mixtures of untreated PTR glass with pure crystalline NaF. XRD traces were recorded under the same operational conditions for both heat-treated samples and standard mixtures of NaF and glass. The volume fraction of crystallized NaF was then recalculated to weight percent using glass and crystal densities. Figure 5 shows α_{eq} in wt% plotted as a function of heat treatment temperature. Recall that heat treatment time for each temperature was not less than that needed to achieve $T_{g/s}$. For temperatures higher than $\sim 745°C$, all NaF is dissolved in PTR melt, i.e. no crystalline phase was detected. This temperature threshold, assigned here as T_{ds} (dissolution temperature), was also verified by optical microscopy and SEM in terms of the presence or absence of crystals under various scales of observation. Therefore, at temperatures higher than T_{ds} the effect of crystallization on T_g should halt, corroborating the data in Fig. 3.

IV. Discussion

Localized precipitation of nano-sized NaF crystals is the main process underlying the optical applications of PTR glass. Therefore, knowledge on the solubility of NaF crystals and its temperature dependence is crucial for understanding and controlling crystallization kinetics in this system. By knowing the equilibrium fraction of crystalline phase and the composition of the parent glass, one can estimate the equilibrium content of NaF dissolved in the glass melt, i.e. the solubility of NaF as

$$\chi_{NaF} = \frac{(C_{NaF}100 - 100\alpha_{eq})}{(100 - \alpha_{eq})} \quad (1)$$

where α_{eq} is the equilibrium concentration of NaF crystals, and C_{NaF} is the concentration of NaF in the parent glass, both on weight basis. A plot of the solubility of NaF in weight percent as a function of temperature is presented in Fig. 6. As for most solids, the solubility of NaF in PTR glass increases with increasing the temperature, i.e. progressively more of the crystalline phase formed at a lower temperature goes back into the melt. Figure 7 shows the same data together with the solubility of NaF calculated via the Schroeder—van Laar equation[16]:

$$\ln \chi = \frac{\Delta H_m (T - T_m)}{RTT_m} \quad (2)$$

which relates the solubility of a solid at a temperature T with its melting enthalpy, ΔH_m, and melting temperature T_m. The melting enthalpy used was $\Delta H_m = 33.35$ kJ/mol.[17] It should be reminded that this equation is valid only for ideal solutions and for a temperature-independent melting entropy. To a fair approximation, silicate glasses and their melts "can be considered as solutions of the salt-like products of interaction between the constituent oxides," as quoted from Shakhmatkin *et al.*[18] Nevertheless, the solubility of NaF in PTR glass calculated using Eq. (2), shown in Fig. 7, provides credible idea about its temperature dependence. After dissolution of NaF, fluorine forms different assemblages with various melt components. These assemblages can be revealed by structural techniques,[19,20] and quantitatively predicted via a thermodynamic approach.[21,22]

The following consideration is relevant for the overall understanding of NaF crystallization in PTR glass. At T_{ds}, the temperature where all NaF is dissolved, the solubility of NaF equals

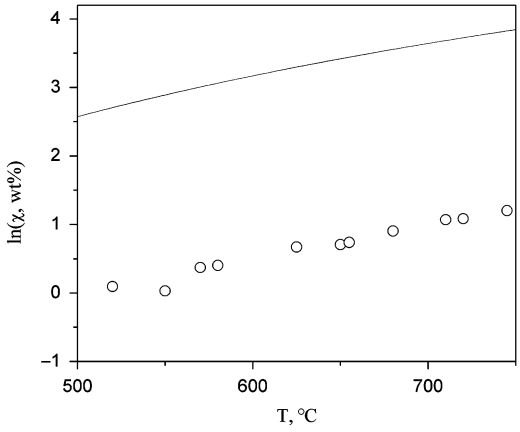

Fig. 7. Solubility of NaF in the glass as a function of heat treatment temperature, together with calculated solubility using Eq. (2) (continuous line) with $\Delta H_m = 33.35$ kJ/mol and $T_m = 1269$ K.

the content of NaF in the parent glass, C_{NaF}. Above T_{ds}, NaF does not crystallize regardless the heat treatment time applied. Decreasing the temperature from T_{ds} leads to increase of supersaturation of NaF in the melt and, hence, to an increase of the thermodynamic driving force for nucleation and growth of NaF crystals. By changing C_{NaF}, one can change T_{ds}, which is higher the higher is C_{NaF}. For the composition of PTR glass investigated in the present study, $T_{ds} \cong 745°C$. As the crystallized volume increases at $T < T_{ds}$, the supersaturation of PTR melt, regarding the NaF content, decreases. When the NaF content in the residual melt reaches the solubility corresponding to that temperature ($T < T_{ds}$), crystallization stops and the crystallized volume remains unchanged, in equilibrium with the dissolved NaF. This equilibrium volume of crystalline phase increases with decreasing the temperature. For the PTR glass composition studied here, the solubility of NaF approaches zero at $T \cong 430°C$. As follows from discussions above, the thermodynamic driving force for crystallization depends not only on the temperature (as in the case of stoichiometric crystallization) but also on the evolution of the crystallization process that leads to a decrease of supersaturation. As shown in Souza *et al.*,[6] a decrease in supersaturation caused a sharp decline in NaF crystal growth in PTR glass during isothermal heat treatment. Nucleation rate is to a great extent more sensitive to supersaturation than crystal growth rate. This is the reason why preliminary growth of crystals and hence decrease of supersaturation in diffusion zones can suppress or completely halt the succeeding NaF nucleation in those zones, as observed in Souza *et al.*[6] Volatilization of fluorine also leads to decrease in supersaturation in a thin surface layer, suppressing crystallization in that layer.[6,23]

One should recollect that the commonly accepted scheme assumes heterogeneous nucleation of NaF catalyzed by the preliminary precipitated silver clusters. But, as already noted, PTR glass without Ag also undergoes volume crystallization of NaF. The accepted scheme was idealized for PTR glass after exposure to UV light. However, in any case, if the thermodynamic driving force for crystallization of NaF approaches zero (i.e., for $T > T_{ds} = 745°C$) the formation of NaF crystals is thermodynamically impossible, and hence any other factors that could foster crystallization (e.g., Ag crystalline clusters) will not be able to play their part in the crystallization process.

The fact that PTR glass also undergoes simultaneous liquid–liquid phase separation was expected because the main components of this glass are silicon and sodium oxides (15 mol% Na_2O and 70 mol% SiO_2). The critical point of the immiscibility dome in the Na_2O–SiO_2 system corresponds to 7.5 mol% Na_2O at 835°C.[24] Fluorine can extend the immiscibility range.[8] Thus, the following question arises—to what glass phase (SiO_2-rich droplets or the matrix glass) does the above estimated solubility relate? The evolution of glass transition temperature at 650°C (Fig. 2) allows one to separate, to some extent, the kinetics of liquid phase separation from that of NaF crystallization. T_g values presented in Fig. 2 relate to the glass matrix, which has the lowest viscosity (and lowest T_g). It seems that initially the kinetics of liquid–liquid phase separation is faster than that of NaF crystallization. This leads to a hasty decrease of T_g during the initial stages of phase transitions in PTR glass. The fact that after passing beyond the trough, T_g strongly increases with increasing the volume fraction of NaF crystals gives us indirect evidence of the crystallization in the glass matrix (and not in the droplets), because the formation of NaF crystals renders the glass matrix poorer in Na and F, i.e. with higher T_g. SEM/SE images of PTR glass heat treated at 520°C for 7.5 h are shown in Fig. 8. These are fracture surfaces unetched (a) and etched with HF (b). The unetched fracture surface reveals only isolated (~200 nm) branching of NaF crystals (arrowed) protruding out of the surface. The time necessary for all NaF allowed by the solubility for this temperature to crystallize is over 90 h, which means that only a fraction of crystallization is achieved after 7.5 h treatment at 520°C. After etching the sample with HF, it is possible to clearly identify rounded (~50 nm) features (boxed in Fig. 8(b)) among the holes left after washing away of the crystalline regions and their surrounding diffusion zones.[6] The rounded features are regarded as liquid–liquid phase separation structure, or the droplet phase. As a result, one can conclude that NaF crystals nucleate and grow in the continuous (matrix) glass, and not in the droplet phase. This finding corroborates earlier proposal from Zanotto and colleagues[25–27] using other glasses.

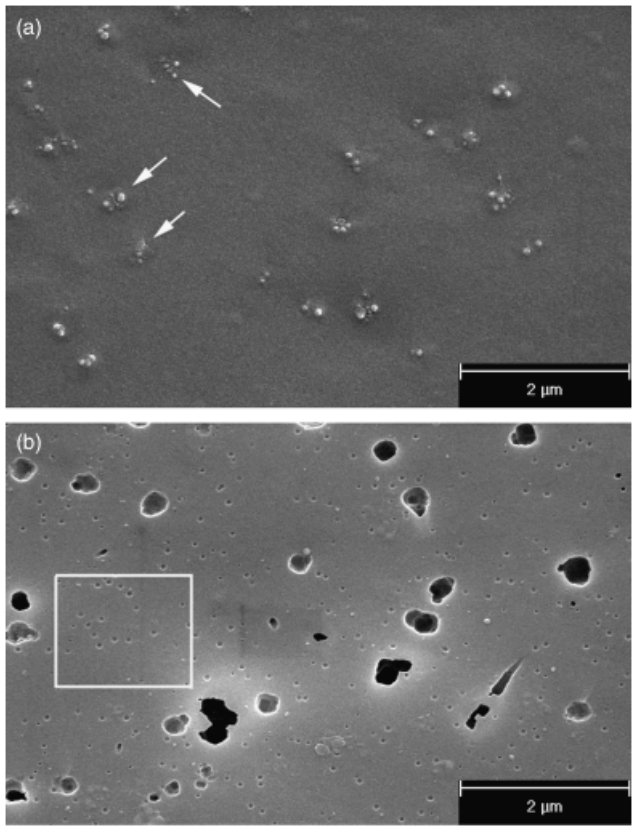

Fig. 8. Scanning electron microscopy/secondary electron images of photo-thermo-refractive glass heat treated at 520°C for 7 h and 30 min. (a) Unetched; (b) etched with hydrofluoric acid.

The crystal size for the sample heat treated at 520°C for 7.5 h (Fig. 8(a)) is significantly smaller than that for the glass samples shown in Fig. 1, heat treated at 650° and 700°C. On the other hand, the crystal number density is dramatically larger for the sample heat treated at 520°C. This gives us some early knowledge on the NaF nucleation kinetics. Also, it is reasonable to expect that liquid–liquid phase separation leads not only to increase in the amount of sodium in the glass matrix, but also of fluorine that can enhance NaF nucleation. Strictly speaking, the composition C_{NaF} in Eq. (1) should be corrected taking into consideration the extra NaF supplied to the glass matrix during liquid phase separation, and the extent of such correction increases with decreasing heat treatment temperature. For that it would be necessary to know the binodal of PTR glass in a wide temperature-composition interval. Such data is, to our knowledge, nonexistent. Conversely, such correction should not be strong because the volume fraction of droplet phase is only a few percent. It is also necessary to recap the role of bromine when discussing solubility of NaF in PTR glass. In Glebova *et al.*[28] it was found that decrease of bromine content in PTR glass drastically suppresses crystallization of NaF, which could be, in the context of the present solubility study, correlated with a decrease in supersaturation of NaF.

By merging data on $T_{g/s}$ (Fig. 3) and χ (Fig. 6), one can derive the dependence of T_g on NaF content in PTR glass, as shown in Fig. 9. The glass, in this case, can be assumed as the matrix glass. The presence of NaF expectedly causes a strong decrease in T_g and hence in viscosity of such glass. This finding corroborates

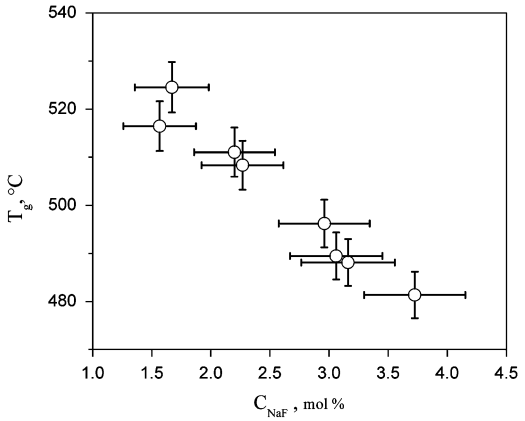

Fig. 9. Glass transition temperature as a function of the NaF concentration in the glass matrix.

literature data[9,29] and may be a valuable tool to assess the NaF content of the glass, which causes major impact on the optical properties of DOEs fabricated with PTR glass.

The increase in NaF solubility in PTR glass with increasing the temperature provides concrete evidence of a physical limit for the total NaF crystallized as a function of temperature, which is different from the actual NaF content in the parent glass. It is also important to take into account that higher crystallized fraction of NaF could be achieved by heat treating the glass at a lower temperature. In Fig. 6 it was shown that, theoretically, all NaF in the glass studied could be turned into crystals at $T \leq 430$°C, where supersaturation of the glass in NaF approaches its maximal value close to C_{NaF} in the parent glass. It leads to strong increase of the thermodynamic driving force for NaF crystallization. However, NaF crystallization at those temperatures below T_g is expected to be very slow due to marked kinetic barrier. Finally, together with the problem of liquid–liquid phase separation, crystal nucleation and overall crystallization kinetics, which will be dealt with in detail in future publications, the solubility of NaF in PTR glass must be carefully considered for designing enhanced heat treatment steps within the framework of controlled microstructural development for better performance of optical devices.

V. Conclusions

In this study, the solubility of NaF in PTR glass as a function of temperature was determined on the basis of the equilibrium volume fraction of crystallized NaF. The temperature above which all NaF originally contained in the parent glass dissolve in the melt, as well as that below which all NaF can be turned into crystals, were estimated. Besides crystallization, PTR glass reveals liquid immiscibility. Interplay between these two processes results in a minimum on the time dependence of the glass transition temperature. The solubility data here produced can be used for estimating the thermodynamic driving force for NaF crystallization, as well as for redesigning chemical composition, thermal processing, and ultimately the microstructure of optical elements based on PTR glass.

Acknowledgments

E. D. Z. acknowledges Brazilian funding agencies CNPq, CAPES, and FAPESP (contract no. 2007/08179-9). G. P. S. and V. M. F. acknowledge FAPESP, contracts no. 2008/02645-0 and 2008/00475-0, respectively. The authors wish to acknowledge valuable comments by Prof. Jean-Louis Souquet.

References

[1]L. B. Glebov, "Photochromic and Photo-Thermo-Refractive (PTR) Glasses"; pp. 770–80 in *Encyclopedia of Smart Materials*. Vol. 2, Edited by M. Schwartz. John Wiley & Sons, New York, 2002.

[2]S. D. Stookey, "Photosensitive Glass, a New Photographic Medium," *Ind. Eng. Chem.*, **41**, 856–61 (1949).

[3]V. A. Borgman, L. B. Glebov, N. V. Nikonorov, G. T. Petrovskii, V. V. Savvin, and A. D. Tsvetkov, "Photothermal Refractive Effect in Silicate Glasses," *Sov. Phys. Dokl.*, **34**, 1011–3 (1989).

[4]L. B. Glebov, V. I. Smirnov, C. M. Stickley, and I. V. Ciapurin, "New Approach to Robust Optics for HEL Systems in Laser Weapons Technology III"; pp. 101–9 in *Proceedings of SPIE*, Vol. 4724, Edited by W. E. Tompson, and P. H. Merritt, SPIE, Orlando, 2002.

[5]J. Lumeau, L. Glebova, L. B. Glebov, V. Golubkov, and E. D. Zanotto, "Origin of Crystallization Induced Refractive Index Changes in Photo-Thermo-Refractive Glass," *Opt. Mater.* **32**, 139–46 (2009).

[6]G. P. Souza, V. M. Fokin, E. D. Zanotto, J. Lumeau, L. Glebova, and L. B. Glebov, "Micro and Nanostructures in Partially Crystallized Photo-Thermo-Refractive Glass," *Phy. Chem. Glasses*, **50**, (2009), doi: 10.1016/j.optmat.2009.07.007.

[7]D. G. Burnett and R. W. Douglas, "Liquid–Liquid Phase Separation in Soda–Lime–Silica System," *Phys. Chem. Glasses*, **11** [5] 125–35 (1970).

[8]J. H. Markis, K. Clemens, and M. Tomozawa, "Effect of Fluorine on the Phase Separation of Na_2O–SiO_2 Glasses," *J. Am. Ceram. Soc.*, **64** [1] C20 (1981).

[9]E. M. Rabinovich, "On the Structural Role of Fluorine in Silicate-Glasses," *Phys. Chem. Glasses*, **24** [2] 54–6 (1983).

[10]A. A. Kiprianov and N. G. Karpukhina, "Oxyhalide Silicate Glasses," *Glass Phys. Chem.*, **32** [1] 1–27 (2006).

[11]A. Prabhu, G. L. Fuller, and R. W. Vest, "Solubility of RuO_2 in a Pb Borosilicate Glass," *J. Am. Ceram. Soc.*, **57** [9] 408–9 (1974).

[12]L. J. Manfredo and R. N. McNally, "Solubility of Refractory Oxides in Soda-Lime Glass," *J. Am. Ceram. Soc.*, **67** [8] C155–8 (1984).

[13]C. W. Kim, K. Choi, J. K. Park, S. W. Shin, and M. J. Song, "Enthalpies of Chromium Oxide Solution in Soda Lime Borosilicate Glass Systems," *J. Am. Ceram. Soc.*, **84** [12] 2987–90 (2001).

[14]P. L. Roeder and I. Reynolds, "Crystallization of Chromite and Chromium Solubility in Basaltic Melts," *J. Petrol.*, **32** [5] 909–34 (1991).

[15]A. Monshi and P. F. Messer, "Ratio of Slopes Method for Quantitative X-Ray-Diffraction Analysis," *J. Mater. Sci.*, **26** [13] 3623–7 (1991).

[16]I. Prigogine and R. Defay, *Chemical Thermodynamics*. Longmans Green, London, 1953.

[17]H. Mediaas, P. Chartrand, O. Tkatcheva, A. D. Pelton, and T. Ostvold, "Thermodynamic Phase Diagram Calculations and Cryoscopic Measurements in the NaCl–$CaCl_2$–$MgCl_2$–CaF_2 System," *Can. Metall. Q.*, **40**, 13–32 (2001).

[18]B. A. Shakhmatkin, N. M. Vedishcheva, and A. C. Wright, "Can Thermodynamics Relate the Properties of Melts and Glasses to their Structure," *J. Non-Cryst. Solids*, **293**, 220–6 (2001).

[19]Y. Sasaki, H. Urata, and K. Ishii, "Structural Analysis of Molten Na_2O–NaF–SiO_2 System by Raman Spectroscopy and Molecular Dynamics Simulation," *ISIJ Int.*, **43** [12] 1897–903 (2003).

[20]B. O. Mysen, G. D. Cody, and A. Smith, "Solubility Mechanisms of Fluorine in Peralkaline and Meta-Aluminous Silicate Glasses and in Melts to Magmatic Temperatures," *Geochim. et Cosmochim. Acta*, **68** [12] 2745–69 (2004).

[21]B. A. Shakhmatkin, N. M. Vedishcheva, and A. C. Wright, "Thermodynamic Modelling of the Structure of Oxyhalide Glasses," *J. Non-Cryst. Solids*, **345**, 461–8 (2004).

[22]D. Dolejš and D. R. Baker, "Thermodynamic Modeling of Melts in the System Na_2O–$NaAlO_2$–SiO_2–F_2O_1," *Geochim. et Cosmochim. Acta*, **69** [23] 5537–56 (2005).

[23]J. Lumeau, A. Sinitskii, L. Glebova, L. B. Glebov, and E. D. Zanotto, "Method to Assess the Homogeneity of Partially Crystallized Glasses: Application to a Photo-Thermo-Refractive Glass," *J. Non-Cryst. Solids*, **355**, 1760–8 (2009).

[24]W. Haller, D. H. Blackburn, and J. H. Simmons, "Miscibility Gaps in Alkali-Silicate Binaries—Data and Thermodynamic Interpretation," *J. Am. Ceram. Soc.*, **57** [3] 120–6 (1974).

[25]E. D. Zanotto, P. F. James, and A. F. Craievich, "The Effects of Amorphous Phase Separation on Crystal Nucleation Kinetics in BaO–SiO_2 Glasses. Part 3: Isothermal Treatments at 718–760°C, SAXS Results," *J. Mat. Science*, **21**, 3050–64 (1986).

[26]E. D. Zanotto and P. F. James, "The Compositional Dependence of Crystal Nucleation in Li_2O–SiO_2 Glasses," *Glastech. Ber.*, **56k**, 794–9 (1983).

[27]A. F. Craievich, E. E. Zanotto, and P. F. James, "Kinetics of Sub-Liquidus Phase Separation in Silicate and Borate Glasses. A Review," *Bull. Soc. Franc. Min. et Crist.*, **106**, 169–84 (1983).

[28]L. Glebova, J. Lumeau, M. Klimov, E. D. Zanotto, and L. B. Glebov, "Role of Bromine on the Thermal and Optical Properties of Photo-Thermo-Refractive Glass," *J. Non-Cryst. Solids*, **354**, 456–61 (2008).

[29]A. A. Kiprianov, N. V. Golubko, N. G. Karpukhina, and V. A. Molodozhen, "Thermal, Electrical, and Potentiometric Characteristics of Sodium Aluminosilicate Glasses with Fluoride Additives," *Glass Phy. Chem.*, **24** [4] 350–4 (1998). □